

# Modeling the heart-brain connection using innovative organ-on-a-chip technology

M.M. Pasterkamp

Committee:

Dr. V. Schwach (AST) - Chairperson

L. Koch MSC (AST) - Daily Supervisor

C. Cofino Fabres MSC (AST) - Daily Supervisor

Dr. Ir. J. Rouwkema (EOST) - External Member

University of Twente

## Abstract

With organ- on- a- chip (OOC) technology, it is possible to study complex cell interaction *in vitro*. This is important for investigating disease pathophysiology and gives an insight into organ function. Here, the heart-brain connection was investigated by a chip with ventricular cardiomyocytes, hippocampal cerebral organoids and cholinergic neurons (HVB-chip). The cells that were used to model the heart-brain system were derived from Human pluripotent stem cells (hPSCs). In addition, the influence of Nerve Growth Factor (NGF) and inhibitor Ro 08-2750 was investigated. NGF stimulates the morphological differentiation and cellular connection of nerve cells. The HVB-chips were treated with different concentrations of NGF and Ro 08-2750, to analyze the influence of NGF on the connection between vagus nerve cells and heart- and brain cells. Immunostaining was performed to image the cellular connections in the HVB-chips. The control images of HVB-chips are presented in this report. The images of the HVB-chip treated with NGF and Ro 08-2750 will be presented in the presentation of this research.

July 7th, 2022

## 1.Introduction

### 1.1 Heart-brain connection

The heart and brain have a special connection in human and animal physiology. Through the sympathetic and parasympathetic branches of the autonomic nervous system, the brain controls the heart directly.(1) With this connection, the cardiac functions respond to inputs from in and outside the body.

In the heart-brain communication, the pathways in the autonomic nervous system are crucial. One pathway is the fibers in the vagus nerve, as seen in figure 1. The vagus nerve, also known as the tenth cranial nerve, promotes cardiac relaxation and contraction. The heart is innervated by the vagus at cardiac muscle cells and at conduction system, also called cardiac plexus. The signals that control the hearts regulation will be sent to the heart's sinoatrial node. (2) The neural output from the cardiac nervous system travels to the brain via ascending pathways.

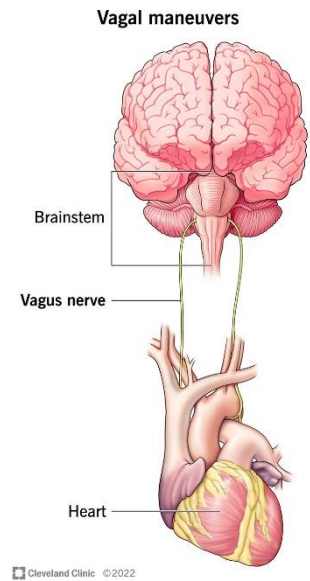


Figure 1: The vagus nerve pathway between the brain and the hart (29)

### 1.2 Cardiac dysfunction and loss of cognitive functioning

Cardiac dysfunction and loss of cognitive functioning are both prominent features of the aging population. In the Netherlands, there are about 1.5 million people with a chronic cardiovascular disease. (3) In addition, the total number of patients suffering from cognitive or cerebral dysfunction is 3.5 million. (4)This number includes patients with migraine, anxiety disorder, mood disorder (including depression), brain injury, dementia, stroke, epilepsy, Parkinson, Multiple Sclerosis, and brain tumors. This provides a certain urgency to do research to get a clearer view of why this is and what to do to make sure this number does not grow further.

There have been many heart-brain studies that investigates the relationships between (cardio-) vascular factors and cognitive impairment.(5) (6)Patients with heart failure, carotid occlusive disease and vascular cognitive impairment were participating in a cohort study. Which concluded that a substantial part of the heart failure and carotid occlusive disease patients had a cognitive impairment. Besides this relation, there has also been done research about the association between cardiac arrhythmias and after having an acute stroke. (7) Cardiac arrhythmias and ECG abnormalities occur frequently in patients with acute stroke, either with or without coexisting cardiac diseases. (8)

### 1.3 Human pluripotent stem cells and cell differentiation

The cells that are used for modeling the heart-brain system are derived from Human pluripotent stem cells (hPSCs).(9) In this research only human embryonic stem cells (hESCs) were used. These hESCs can self-renew indefinitely and have the ability to become almost any cell type in the human body. The heart cells that will be used are cardiomyocytes.(10) The technique that will lead to differentiation of these cells is embryoid body (EB) differentiation. The vagus nerve cells that will be used are cholinergic neurons. The brain cells that will be used are hippocampal cerebral organoids.

#### 1.4 Organ-on-chip technology

There are multiple *in vitro* models based on cardiac cell types differentiated from human pluripotent stem cells (hPSCs). (11)

The first model that has been used was a 2D cell culture. (12) This culture is simple and has low-cost maintenance of cell culture. However, these models are far from physiological conditions and do not provide an environment to immature phenotypes of the hPSCs-derived cells. In contrast, 3D cell culture has more resembling of the physiological conditions and provides a more cellular environment to mature the phenotype of the hPSCs-derived cells. The cell-cell interaction can be relatively more relatable to a *in vivo* model. However, 3D models can not provide a complex interaction between different types of cells, because there is no physical separation between the different cell types. By using organ-on-a-chip (OOC) technology, it is possible to study all cell interaction with physical separation of different cell types. (13) However, OOC has also some disadvantages due the presence of the surface effect. The dimensions of the channels or chamber are relatively small, so the surface around the cell environment effects a relatively high amount of the cells. Besides, OOC provides a relatively accurate insight into the organ function and disease pathophysiology. (14) It makes toxicity screening and target discovery possible for drug testing. That is why OOC is necessary for the development of new drugs and personalized medicines, like for the heart-brain system.

In previous research, there has been developed a heart-on-a-chip and brain-on-a-chip. (11)(15) But there has not been a chip developed with heart, brain and vagus cells on it.

#### 1.5 Stimulating the vagus nerve cells by Nerve Growth Factor

NGF, also known as Nerve Growth Factor, stimulates morphological differentiation of nerve cells. (16) It also regulates neuronal gene expression through interaction with specific cellular receptors. In addition to that, NGF plays a critical role in mature neurons. It is stimulating for maintaining their function and phenotype. Findings in other studies led to the hypothesis that purified NGF might be useful to prevent nerves from degeneration. (17) Moreover, studies demonstrated that NGF can promote survival, differentiation, and functional activity of sensory and sympathetic nerve cells. Other studies revealed that NGF exerts a critical protective action on specific brain cells, non-neural and neoplastic cells. (17,18) NGF has also influence on the cardiac sympathetic nerves and the myocardium. (19)

NGF binds to two different receptors,  $trkA^{NGFR}$  and  $p75^{NTR}$ . (20)  $p75^{NTR}$  is a non-selective neurotrophin receptor and  $trkA^{NGFR}$  is a tyrosine kinase receptor.  $p75^{NTR}$  controls the neural cell survival, cell differentiation or apoptosis. The binding of  $p75^{NTR}$  is depended on the expresion of  $trkA^{NGFR}$ , a lack of expression will cause apoptosis. The interaction between the two NGF receptors and NGF can be inhibited in two levels. First, by NGF conformation, to make sure NGF is no longer recognized by the receptors. Secondly, by blocking the binding site of  $trkA^{NGFR}$  and  $p75^{NTR}$ . These forms of inhibition will be investigated by using Ro 08-2750 as inhibitor for NGF. The hypothesis is that this will causes decrease in differentiation of the vagus nerve cells or it will lead to apoptosis. Therefore, the heart and brain cells cannot have a cellular interaction with the vagus nerve cells. It further causes no heart-brain connection on the chips, only heart and brain cells individually.

## 1.6 State model

Modeling the heart-brain axis by OOC-technology is a long-lasting process. First the heart-vagus nerve-brain chips (HVB-chips) were optimized. The conditions for the chip fabrication, the used coatings and cell seeding were checked before starting treatments on the HVB-chips. During this research, the first round of HVB-chips was only treated with a maintenance medium to study the development of each cell type and the cellular interaction. This was evaluated by performing immunostaining. The antibodies were first tested out on only EB-cells, to check the concentrations and the expression of the antibodies. After optimizing the HVB-chips, the HVB-chips were treated with NGF and inhibitor Ro 08-2750. The concentration of NGF has been found in earlier studies. (21) The concentration of inhibitor Ro 08-2750 was determined by doing a cell viability test. Hereafter, the HVB-chips were treated for 10 days under different conditions. Immunostaining was also performed to evaluate.

## 1.7 Aim of this research

The aim of this research was to model the heart-brain connection by using OOC-technology. In addition, the influence of NGF and inhibitor Ro 08-2750 was investigated to ascertain if NGF will promote the differentiation and cellular connection of VN-cells in the HVB-chip.

## 2. Methods

### 2.1 Method differentiation BO-, EB- and VN-cells

#### 2.1.1 Maintenance culture of hESCs

For all the differentiation processes the same maintenance of culture of hESCs has been used. The hPSCs were maintained as undifferentiated colonies and added to wells with E8 (Essential 8 stem cell medium) and vitronectin as coating reagent.(10) Twice a week, the hPSCs in E8 were passaged with 0.5 mM EDTA and cryopreserved in E8 cryopreservation medium. The circumstances of the stem culture were 37 C, 5% CO<sub>2</sub> and humidified.

#### 2.1.2 EB differentiation

The cardiac EBs that were used on the HVB-chip are made by spin-EB-based differentiation of ventricular cardiomyocytes (VMs) from hPSCs grown in defined cultures as indicated in (22). The hPSC-line that was used is the double-reporter human embryonic stem cell (hESC) line (HES3) carrying both the Green Fluorescent Protein (GFP) at the NKX2.5 genomic locus(23) and mRubyII fused to the cardiac sarcomeric protein  $\alpha$ -actinin (ACTN2; DRRAGN (23)). To generate EBs from hPSCs, the hPSCs were resuspended in EB formation medium and seeded in wells. The day after the hPSCs were aggregated, the EBs resuspended in cardiac mesoderm induction medium. Cardiac mesoderm was induced with growth factors to stimulate the differentiation of the hPSCs, the growth factors are activin-A, bone morphogenetic protein 4 (BMP4), the small molecule inhibitor of glycogen synthase kinase-3 $\beta$  (CHIR-99021), vascular endothelial growth factor (VEGF) and stem cell factor (SCF) in BPEL medium(22). At day 3, 7 and 10 the EBs were refreshed with plain medium. On day 14, the EBs were refreshed with Cardiomyocyte maintenance medium, see Table 1, till further use in the HVB- chip.

#### 2.1.3 BO differentiation

The BOs that were used for the HVB-chip were differentiated hPSCs into hippocampal brain tissue. (24) The hPSC-line that was used is H9. The first step in the differentiation process was dissociating the hPSCs colonies into single cells. The cells were transferred and neutralized. After centrifugation and resuspension, the cells were counted and seeded with E6-medium + ROCK inhibitor. The next day, the wells were changed to E6 medium with 2 $\mu$ M XAV939 as WNT inhibitor and 10  $\mu$ M SB431542 and 500nM LDN193189 as the dual SMAD inhibitors (E6 + SMAD + WNTi). The medium was changed every day (E6 + SMAD + WNTi) until day 6. After day 6 the cells, the spheroids, were embedded in Matrigel. The neuroepithelial EBs were embedded into Matrigel for further differentiation. On day 10 of differentiation the Brain organoid maintenance medium was added, see Table 1. The BO- cells were refreshed till further use in the HVB-chip

### 2.1.4 VN differentiation

The VNs that were used on the HVB-chips were differentiated hPSCs into cholinergic neurons. (25) For the differentiation of VN-cells, also hPSCs-line H9 cells were used. These ESCs were first differentiated into vagal NCCs by using KSR medium (KnockOut DMEM and 15% KnockOut Serum Replacement) and N2 medium (DMEM HEPES, 1% Penicillin-Streptomycin, and 10 µg/ml N2 supplement) for 12 days. Next, the vagal NCCs were cultured in the form of floating spheroids for four days. After the spheroid formation the cells did undergo cholinergic neuron induction and cholinergic neuron maturation. On day 16 of differentiation the Vagus Nerve maintenance medium was added, see Table 1. The VN- cells were refreshed till further use in the HVB-chip

### 2.2 Maintenance mediums

In Table 1 the components of the different maintenance media are seen. These media were used for the refreshments of the individual cells and the HVB-chips.

**Table 1: Maintenance Media of BO-, VN- and EB-cells**

| Brain Organoid maintenance Media (BOM- medium) | Vagus Nerve maintenance Media (VN-medium) | Cardiomyocyte maintenance Media (CM-medium)              |
|--|---|--|
| 50% DMEM/F-12                                  | 10 µg/ml N2 supplement                    | 111 mM Na Dulbecco's Modified Eagle's Medium             |
| 50% mL Neurobasal                              | 20 µl/ml B27 supplement                   | 15 mM D(+)- Glucose                                      |
| 0.5x N2 supplement                             | 10 µg/ml Glutamax                         | 0.19 mM Sodium 3-hydroxybutyrate                         |
| 1x Glutamax                                    | 10 µg/ml MEM Nonessential Amino Acids)    | 0.5 mM L-Carnitine Hydrochloride                         |
| 0.025% Insulin                                 | 10 ng/ml BDNF                             | 1mM Creatine monohydrate                                 |
| 0.7 mM MEM-NEAA                                | 100 µM L-Ascorbic Acid                    | 5mM Taurine  |
| 50 U/mL Penicillin-Streptomycin                |   | 31 µM Phenol Red   |
| 55 mM 2-mercaptoethanol (1:500 Gibco)          |   | DI Water   |
| 1x B27 supplement without Vitamin A            |   | 0.5 mM Sodium Pyruvate                                   |
|  |   | 1 xTrace elements A, B, C                                |
|  |   | 1x Chemically defined lipid concentrate                  |
|  |   | 448 µM GlutaMAX Supplement                               |
|  |   | 0,01 x Insulin-Transferrin-Selenium Ethanolamine (ITS-X) |
|  |   | 50 µg/ml Ascorbic acid-2P                                |
|  |   | 0.5 x Penicillin- Streptomycin                           |
|  |   | 0.25% BSA  |
|  |   | 3.7 g/L Sodium hydrogen carbonate (NaHCO <sub>3</sub> )  |
|  |   | 100 nM 3' 5-Triiodo-L_thyronine sodium salt (T3)         |
|  |   | 1 µM Dexamethasone                                       |
|  |   | 100 ng/ml Long R3 IGF-I human (IGF)                      |

### 2.3 Microfluidic chip fabrication

For the microfluidic chip fabrication, a mold was used. The mold consists of multiple compartments, the shape and dimensions are seen in figure 3. The central channel is for the VN cells. This channel is spread over the surface of the chip, with a total length of 6 mm. The central has two openings, both have a diameter of 1 mm. After cell seeding, there were pipette tips in these openings. The central channel is connected to two other chambers, the EBs and BOs were seeded here. Between this connection, heart and brain compartments are connected via microchannels. The EBs and the BOs were not able to go through these channels, but the VN-cells could go through. Both chambers had a diameter of 2 mm, there were also pipette tips placed here to act as medium reservoirs.

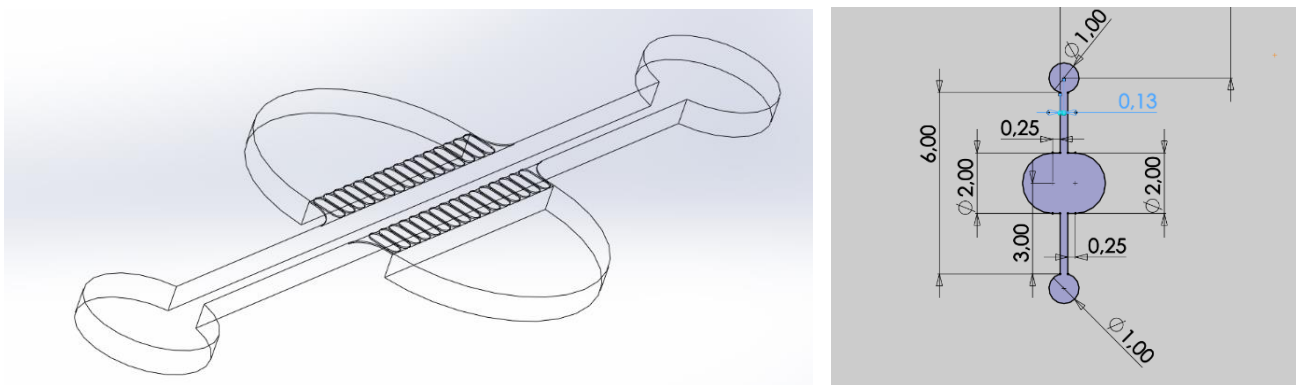


Figure 2: Solidworks design of the used mold. Left the full mold and right the mold with all the dimensions

The chip was made of PDMS mixed with 184 silicone elastomer curing agent as crosslinker. The ratio that is used is 1:10, 15 g of this mixture was used per mold. After filling the mold, the chips were placed in a vacuum chamber for 25 minutes. Thereafter, the chips were left in an oven at 65 degrees for at least three hours. When the chips were fully cured, the channels of the chips were punched. The chips were bonded to the glass surface by plasma treatment, by using Plasma System model CUTE.

Poly-L-Ornithine (PLO) coating to improve cell attachment was added overnight.(26). PLO is diluted with PBS, 15  $\mu\text{g}/\text{ml}$ . The next day after doing a wash step with PBS, the Laminin and Fibronectin coating were added overnight. Laminin and Fibronectin are both extracellular matrix proteins that support adhesion, proliferation, and differentiation of cells. (27)Laminin and Fibronectin were also diluted with PBS, 2  $\mu\text{g}/\text{ml}$ . The chips were ready for cell seeding after this step.

## 2.4 Cell seeding and maintenance of HVB-chips

The VN- cells are the first cells that were seeded on the HVB- chip, this was day 15 to 16 of the VN-differentiation. Before seeding, the VN spheres were washed with PBS and incubated with EDTA for 10 minutes. After this, the cells were placed in VN- medium, without BDNF. Trypan blue, 0,04%, was used for counting the living cells. Therefore, 1,75 million cells/milliliter could be added to the chips. The VN-cells with medium (without BDNF) were incubated for 20 minutes, this allowed the cells to bind to the surface in the chip. After this incubation, the remaining medium was aspirated and new VN-medium was added to all channels. The chips were incubated for a week and every two days the medium was changed with new VN-medium.

After one week, the BOs and EBs were also seeded into the chips. The BOs were seeded between day 24-28 of the differentiation process with transition medium, this medium consisted of DMEM and pen/strep. The EBs were seeded between day 14- 21 of differentiation with cardiac medium, two EBs per chip. HVB-chips, including VN-, BO- and EB-cells were seeded. Also chips with only VN-cells, chips with only BO-cells and chips with only EB-cells were prepared. The HVB-chips were refreshed every two days with new medium. For the VN-cells was this VN-medium, for the BO-cells Bom medium, for the EB-cells CM-medium.

The first round of HVB-chips was used to optimize the conditions and test the immunostaining. The second and third round of HVB-chips will have different conditions, these are seen and explained in 2.6.

## 2.5 Cell Viability Assay

The cell viability is required for knowing which concentration of the Ro 08-2750 suitable for the VN-cells on the HVB-chips. It is also a check if the treatment is toxic to the VN-cells or has a negative impact on the viability. For measuring the cell viability, Cell titer glo 2.0 reagent has been used.(28) This CellTiter-GloR 2.0 reagent was stored in the freezer and thawed at 4 degrees overnight in the fridge. One hour before doing the assay it was put at RT. The VN-cells that were used for the viability assay were from the same batch that were seeded in the chips, they were on day 19 of differentiation. The VN-cells were kept in culture medium in a 96-well plate. In total there were 12 conditions tested, seen in Table 2. Every condition is performed in duplicate, except condition 12 this was in triplicate. The added volume of each condition was 135  $\mu$ l.

**Table 2: Cell viability conditions**

| Condition |                         |
|-----------|-------------------------|
| 1         | 0.01 $\mu$ M Ro         |
| 2         | 0.03 $\mu$ M Ro         |
| 3         | 0.1 $\mu$ M Ro          |
| 4         | 0.3 $\mu$ M Ro          |
| 5         | 1.0 $\mu$ M Ro          |
| 6         | 2.5 $\mu$ M Ro          |
| 7         | 5 $\mu$ M Ro            |
| 8         | 10 $\mu$ M Ro           |
| 9         | VN-medium               |
| 10        | 2 $\mu$ M Staurosporine |
| 11        | 5 ng/ml NGF + 0,1 Mm Ro |
| 12        | 5 ng/ml NGF             |

Every condition has been incubated for 19 hours in the incubator. The plate was set at RT 30 minutes before adding the assay. After 30 minutes, the media of each condition was aspirated. Thereafter, 100  $\mu$ l VN-medium and 100  $\mu$ l CellTiter-GloR 2.0 reagent was added to each well. The contents were mixed for 2 minutes on an orbital shaker and incubated at RT for 10 minutes to stabilize the luminescent signal. After incubation, the contents were transferred to a white 96-plate and ready for recording the luminescence. The results were analyzed in excel. Therefore, the accurate concentrations of the Ro were determined for the HVB-chips.

## 2.6 Treatment chips

For the treatment of the chip, there are 4 conditions used on 4 types of different chips. An overview is seen in Table 2.

**Table 2: Overview all conditions and quantity of the HVB-chips**

| Condition      | Full HVB-chips | VN-chips | BO-chips | EB-chips |
|----------------|----------------|----------|----------|----------|
| Control        | 3              | 1        | 1        | 1        |
| 1.0 $\mu$ M Ro | 4              | 1        | 1        | 1        |
| 2.5 $\mu$ M Ro | 3              | 1        | 2        | 2        |
| 5 ng/ml NGF    | 4              | 2        | 2        | 2        |

The different treatments were added to the maintenance media. The HVB-chips were refreshed with new medium every two days. After 10 days, the HVB-chips were ready for immunostaining.

## 2.5 Fixation and immunostaining

At first, the cells on the HVB-chips were washed with PBS+. The next step was the fixation step. The cells were fixed with fixation solution, consisting of Formalhyde 4% in PBS+. Thereafter the cells were washed again, 3 times 5 minutes. The washing solution consist of 0,3% BSA, 0,01% Triton X-100 in PBS. Thereafter, the permeabilization and blocking buffer

were added and incubated at RT. This buffer consisted of 0.1% Triton X-100, 0.1% Tween20, 5% BSA in PBS+. After removing this buffer, the primary antibody with antibody buffer was added to the chips. The antibody buffer was the same as the permeabilization and blocking buffer. The primary antibody has been incubated overnight at 4 degrees. The next day, the chips were washed 3 times 10 minutes with the washing buffer. The secondary antibody was added with PBS + 1% PBS and incubated 90 minutes at RT. After 3 washing steps of 20 minutes, DAPI with washing buffer was added with the ratio 1:1000. This was incubated for 15 minutes at RT and followed by 3 times 1 minute washing steps. Finally, the chips were left in PBS and ready to be imaged.

The immunostaining was done multiple times, first on only EB-cells. The used antibodies and conditions can be found in Table 3. The primary antibodies were cardiac troponin 1 (CTnT1 CT.), B-adrenergic, cholinergic receptor muscarinic 2 (CHRM2). The secondary antibodies were Alexa Fluor 488 (AF488) and Alexa Fluor 647 (AF647)

**Table 3: primary and secondary antibodies per condition for immunostaining**

| Condition   | Primary antibody  | Secondary antibody                                   |
|-------------|---|--|
| Condition A | 1:250 CTnT1 CT. M $\alpha$ H + 1:50 B-adrenergic Rb $\alpha$ H  | 1:500 AF488 G $\alpha$ M + 1:500 AF647 G $\alpha$ Rb |
| Condition B | 1:250 CTnT1 CT. M $\alpha$ H + 1:100 B-adrenergic Rb $\alpha$ H | 1:500 AF488 G $\alpha$ M + 1:500 AF647 G $\alpha$ Rb |
| Condition C | 1:250 CTnT1 CT. M $\alpha$ H + 1:50 CHRM2 Rb $\alpha$ H         | 1:500 AF488 G $\alpha$ M + 1:500 AF647 G $\alpha$ Rb |
| Condition D | 1:250 CTnT1 CT. M $\alpha$ H + 1:100 CHRM2 Rb $\alpha$ H        | 1:500 AF488 G $\alpha$ M + 1:500 AF647 G $\alpha$ Rb |

After performing the immunostaining on only EBs, the full optimized HVB-chips were also imaged by immunostaining. The same condition as Table 3 were used, but this causes a blurry image with lot of background coloring. To optimize the staining, 0.1 % Tween 20 was removed from the used buffer. The staining was performed on HVB-chips again, the used antibodies can be found in Table 4.

**Table 4: primary and secondary antibodies per condition for immunostaining**

| Condition   | Primary antibody  | Secondary antibody                                   |
|-------------|---|--|
| Condition E | 1:100 B-tubulin M $\alpha$ M + 1:250 CTnT1 M $\alpha$ H         | 1:500 AF488 G $\alpha$ M + 1:500 AF647 G $\alpha$ Rb |
| Condition F | 1:100 B-tubulin M $\alpha$ M + 1:100 CHRM2 Rb $\alpha$ H        | 1:500 AF488 G $\alpha$ M + 1:500 AF647 G $\alpha$ Rb |
| Condition G | 1:100 B-tubulin M $\alpha$ M + 1:100 B-adrenergic Rb $\alpha$ H | 1:500 AF488 G $\alpha$ M + 1:500 AF647 G $\alpha$ Rb |

### 3. Results

3.1 The conditions with concentration 1.0  $\mu\text{M}$  and 2.5  $\mu\text{M}$  Ro 08-2750 show higher percentage VN-cell viability than the condition with VN-medium

The viability of VN-cells for 12 different conditions are seen in Figure 3. The percentages are normalized to the VN-cells with only medium. Figure 3 shows that using 10  $\mu\text{M}$  Ro 08-2750 causes a relatively high degree of apoptosis, even more than the 2  $\mu\text{M}$  Staurosporin. In contrast, the conditions 1.0  $\mu\text{M}$  Ro 08-2750, 2.5  $\mu\text{M}$  Ro 082750 and 5ng/ml NGF + 0,1  $\mu\text{M}$  Ro 08-2750 show a higher cell viability than VN-medium. Therefore, the condition 1.0  $\mu\text{M}$  and 2.5  $\mu\text{M}$  Ro 08-2750 were chosen to add to the chips.

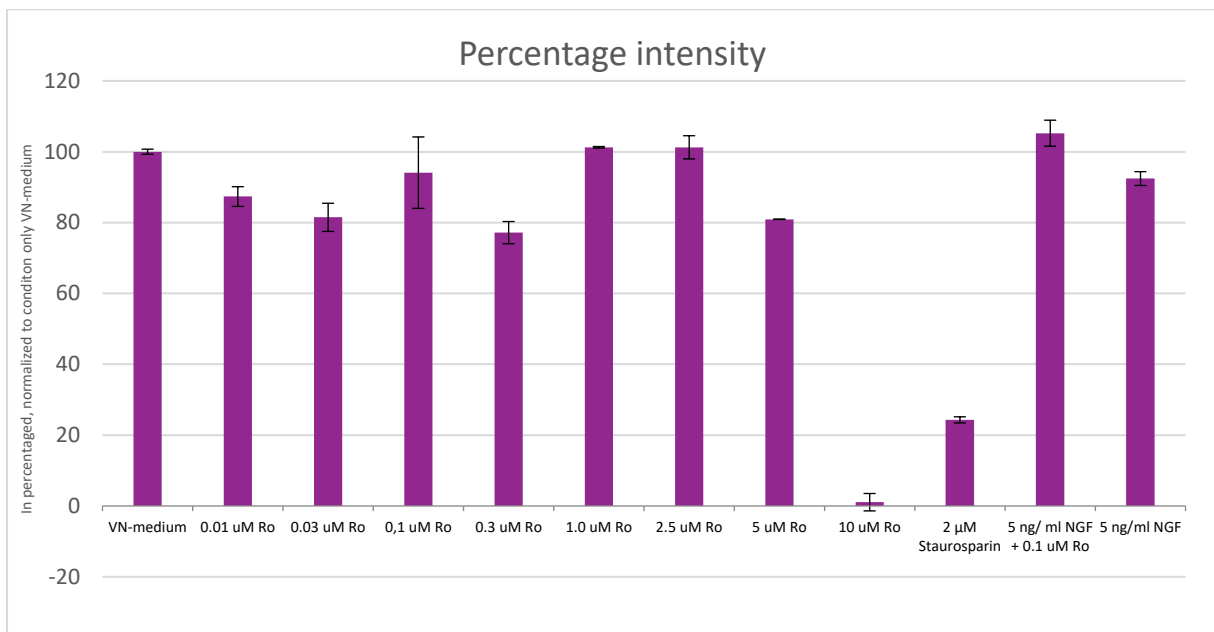


Figure 3: Viability of VN-cells for 12 different conditions

### 3.2 CTnT1 CT, B-adrenergic and CHRM2 express myocardium in cardiac EB-cells

The images for the characterization of the EBs by immunostaining are seen in Figure 4. First, the DAPI shows the nucleus of the individual heart cells. The EBs have a different shape but comparable number of cells, seen through the amount of DAPI expression. The CTnT1 CT has expressed the myocardium of the EBs during contraction. Every condition has the same concentration of CTnT1 CT, seen in Figure 4, condition C and B have relatively more expression than condition A and D. CHRM2 and B-adrenergic both express myocardium of the EBs during relaxation. Both condition B and D have a relatively lower concentration of CHRM2 and B-adrenergic than condition A and C. In contrast, the expression of CHRM2 and B-adrenergic is relatively higher. Generally, Condition C and D have expressed myocardium over the entire EB. Condition A and B have expressed myocardium on the side of the edge of the EBs.

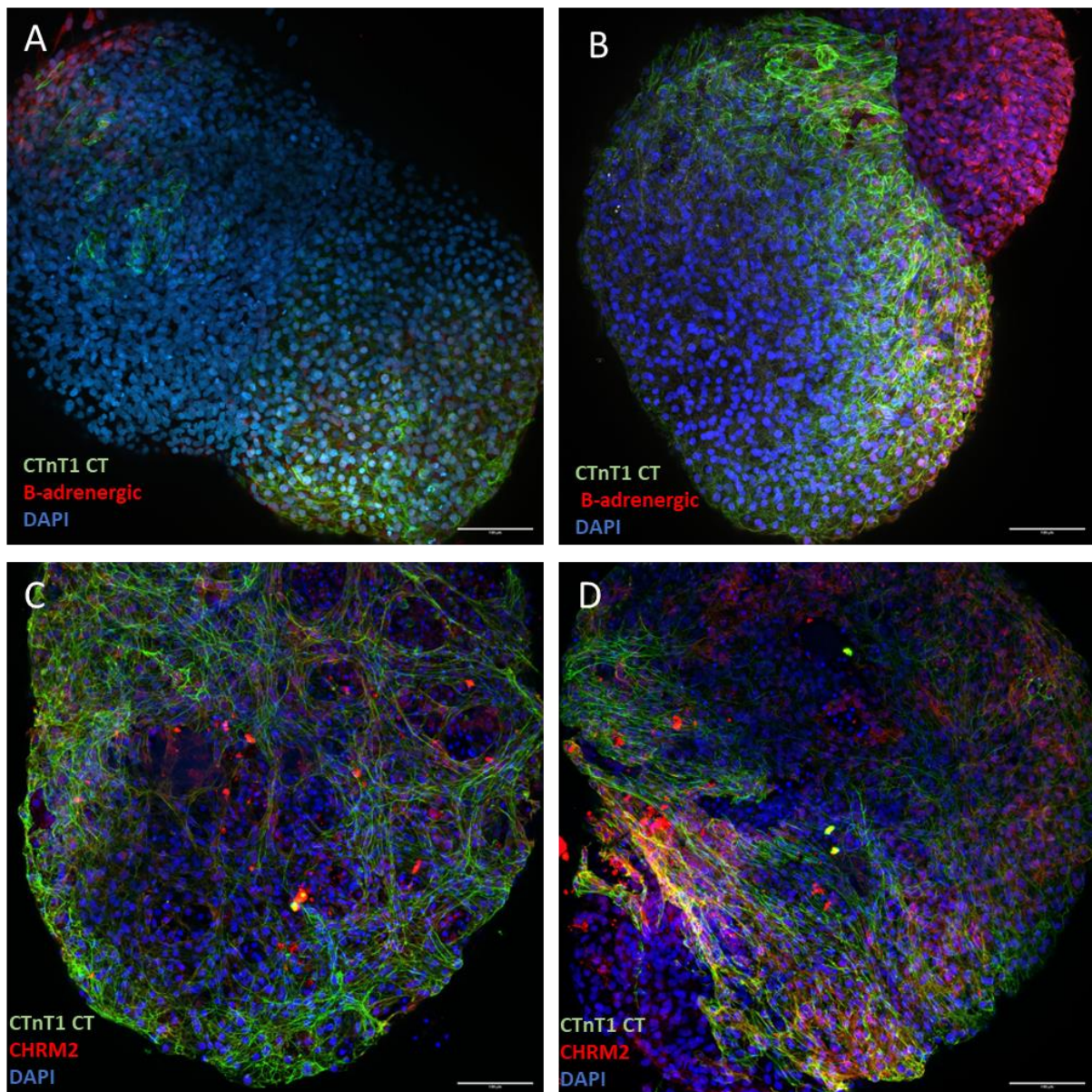


Figure 4: Immunostaining for characterization of EBs. A shows 1:250 CTnT1 CT. + 1:50 B-adrenergic as primary antibodies. B shows 1:250 CTnT1 CT. + 1:100 B-adrenergic as primary antibodies. C shows 1:250 CTnT1 CT. + 1:50 CHRM2 as primary antibodies. D shows 1:250 CTnT1 CT. + 1:100 CHRM2 as primary antibodies. All conditions have 1:500 AF488 + 1:500 AF647 as secondary antibodies. Scale bar = 100  $\mu$ m

### 3.3 Optimized immunostaining for HVB-chips

The protocol of immunostaining HVB-chips has been optimized. To test if the conditions were suitable, the immunostaining was tested two days after cell seeding of HVB-chips.

Figure 5 shows images of a full HVB-chip, including BO-, VN- and EB-cells two days after cell seeding. In A the BO- and VN-cells connection is shown, seen by the B-tubulin expression. The cells are partly connected by elongated extensions, which are the axons of the VN-cells. In B the EB- and VN- cells are shown. The cells here are also partly connected, so there is a connection between the EB- and VN- cells, seen by the B-tubulin and CTnT1 CT expression. The DAPI also shows a high cell density. In C only the EB-cells are shown, seen by the CTnT1 CT expression. There also some green dots seen, because some of the B-tubulin staining got in the CHRM2 channel. In D the VN-cells are seen, there has been a relatively high connection between the cells. There are relatively a lot of elongated extensions seen by the B-tubulin. There is also a relatively high cell density, seen by the DAPI expression.

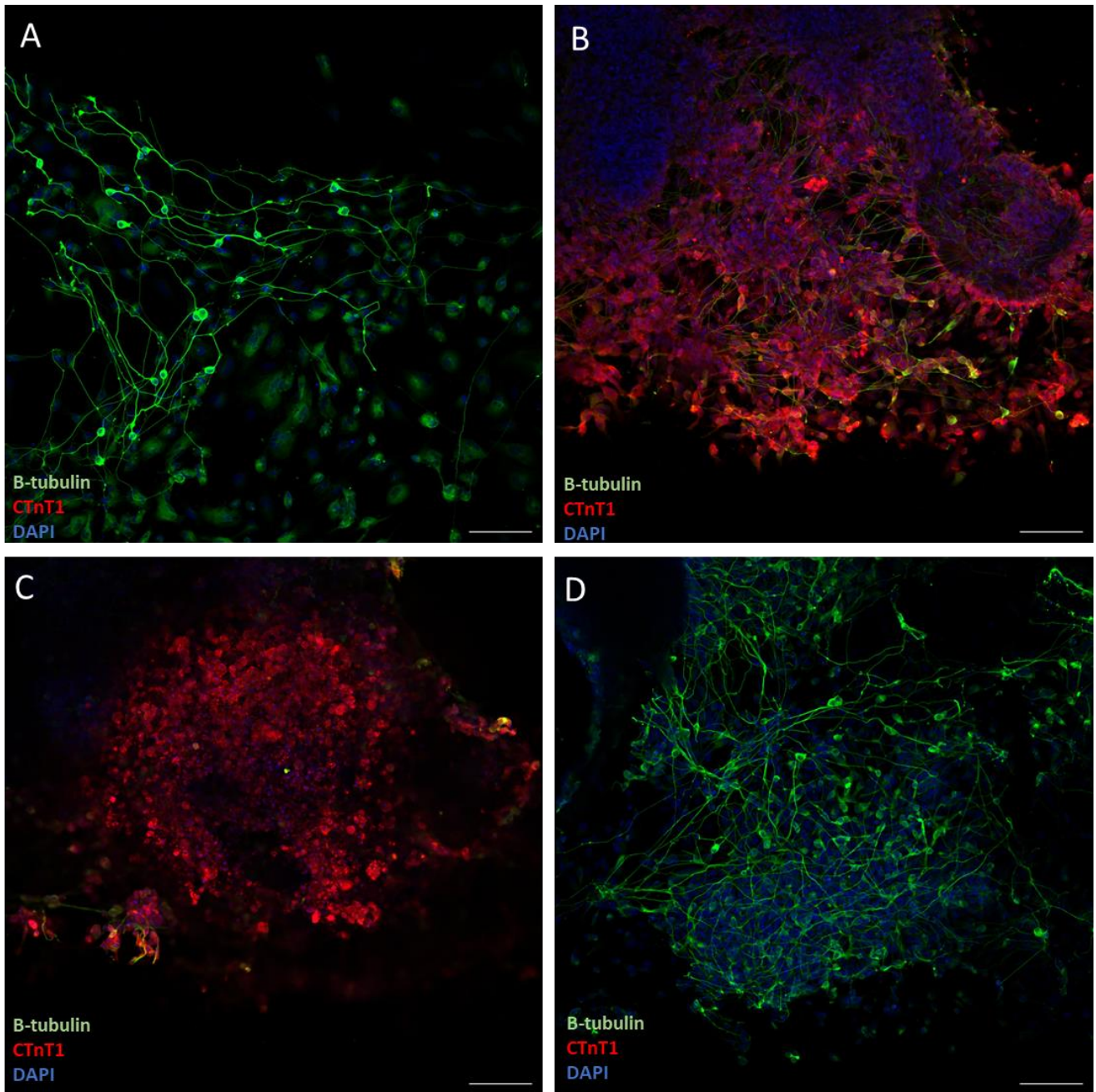


Figure 5: Immunostaining for characterization of HVB-chips. A shows the interaction between BO- and VN- cells. B shows the interaction between EB- and VN-cells. C shows only EB-cells. D shows only VN-cells. All images express 1:100 B-tubulin + 1:250 CTnT1 as primary antibodies and 1:500 AF488 + 1:500 AF647 as secondary antibodies. Scale bar = 100  $\mu$ m.

Figure 6 shows also images of a full HVB-chip. In contrast, there were no BO-cells found during the imaging of the immunostaining. In A only EB-cells are shown, these are expressed by CHRM2. The DAPI also shows a relatively high cell density. The B-tubulin expression shows that there is almost no connection between the EB- and VN-cells. In B only VN-cells are shown, these are expressed by B-tubulin. It shows that there is not much cell interaction by elongated extensions between the individual VN-cells. DAPI shows that there is relatively low cell density.

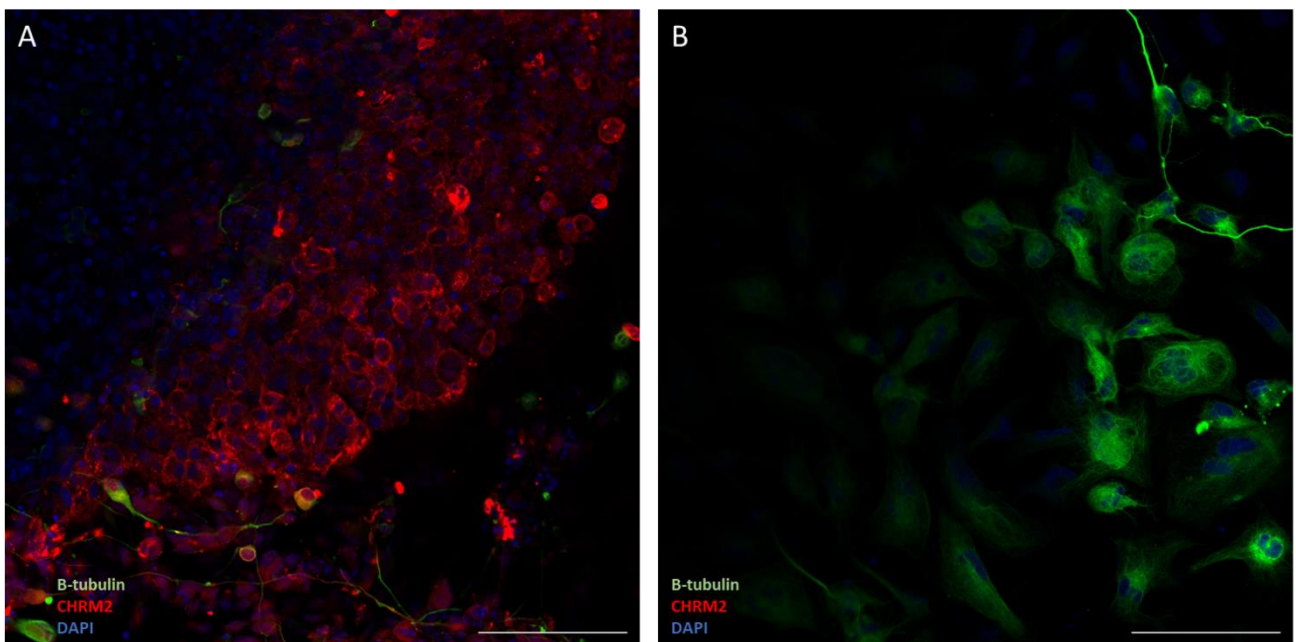
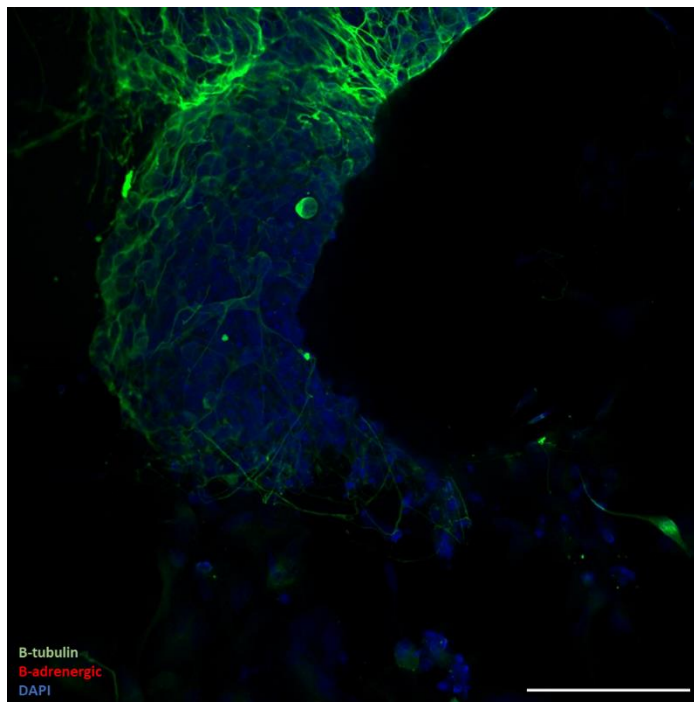


Figure 6: Immunostaining for characterization of HVB-chips. A shows only EB-cells. B shows only VN-cells. Both images express 1:100 B-tubulin + 1:100 CHRM2 as primary antibodies and 1:500 AF488 + 1:500 AF647 as secondary antibodies. Scale bar = 100 µm.

Figure 7 shows only the BO-cells of a full HVB-chip. B-tubulin expresses the cell interaction between the BO-cells. This is only on one side of the BO. DAPI shows that there are relatively many cells without cell interaction.



*Figure 4: Immunostaining for characterization of HVB-chip. It shows only BO-cells. It expresses 1:100 B-tubulin + 1:100 B-adrenergic as primary antibodies and 1:500 AF488 + 1:500 AF647 as secondary antibodies. Scale bar = 100  $\mu$ m.*

### 3.4 Bright-field microscope shows difference between the condition 2.5 $\mu$ M Ro 08-2750 and condition 5ng/ml NGF

In Figure 8 the images of an only cardiac chip are seen of the condition 2.5  $\mu$ M Ro 08-2750 and condition 5ng/ml NGF at day 5 and day 12 after EB-cell seeding. For both conditions, the EBs are more bonded to the chip after 12 days than 5 days. The EBs are also denser and have a relatively better connection with the surrounded VN-cells. For the VN-connection, there is not much difference to see between the two conditions. This can be concluded after doing immunostaining.

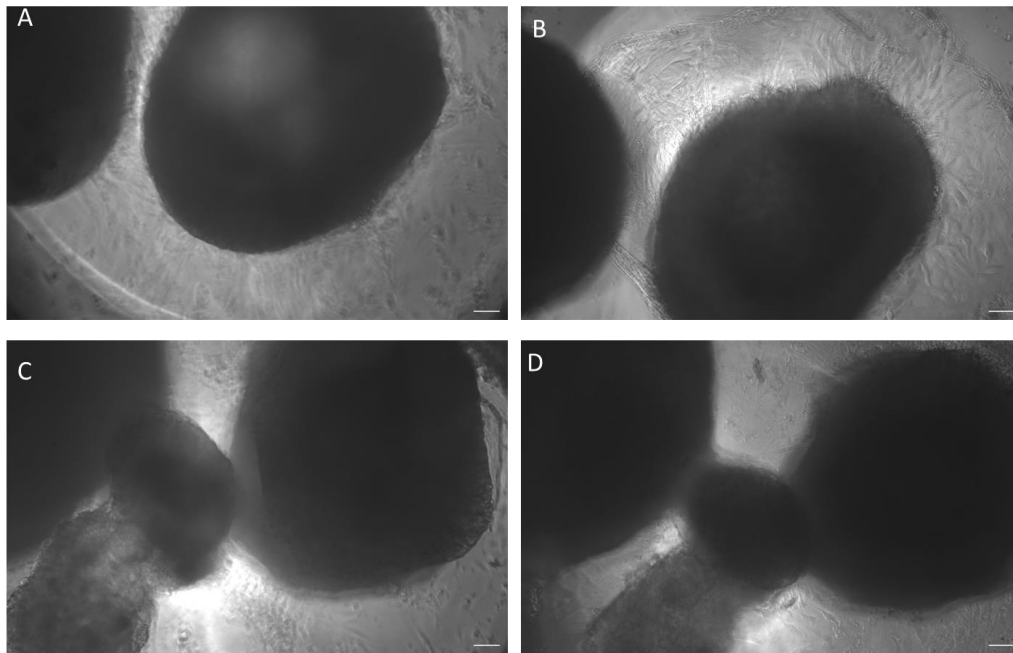


*Figure 8: EB-cell chip. A is condition 2.5  $\mu$ M Ro 08-2750, at day 5 after EB-cell seeding. B is condition 2.5  $\mu$ M Ro 08-2750, at day 12 after EB-cell seeding. C is condition 5ng/ml NGF, at day 5 after EB-cell seeding. D is condition 5ng/ml NGF, at day 12 after EB- cell seeding. Scale bar = 442  $\mu$ m*

In Figure 9 the images of an only BO-cells chip are seen of the condition 2.5  $\mu$ M Ro 08-2750 and condition 5ng/ml NGF conditions at day 5 and day 12 after BO-cell seeding. Both conditions have on day 5 relatively more elongated extensions. After 12 days the BO-cells are more formed to a steroid. The density and connection with the VN-cells cannot be determined with these images. By doing immunostaining this can be concluded and the conditions can be compared.

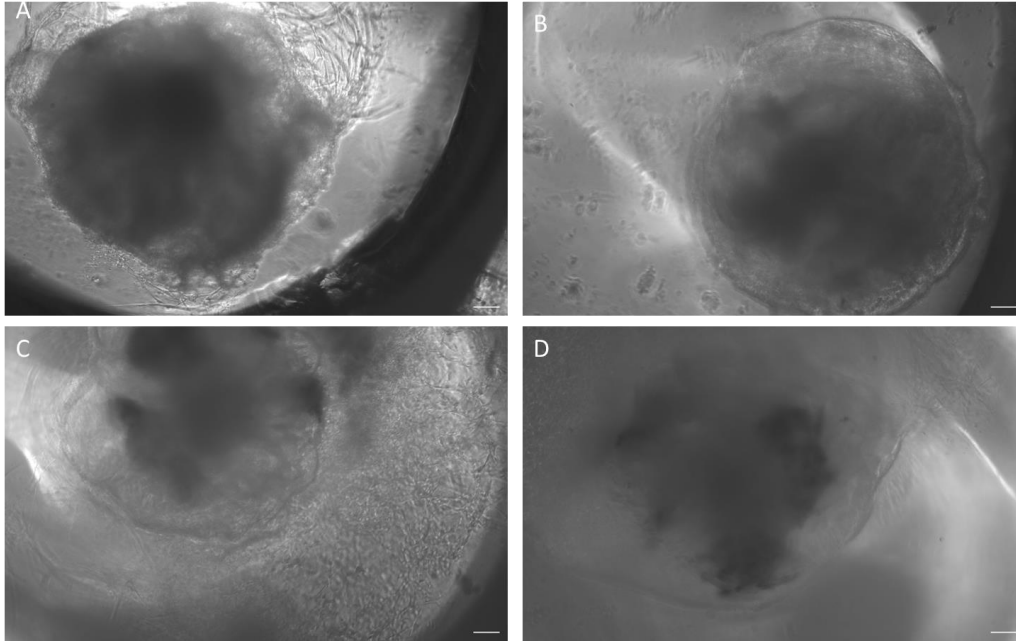


Figure 9: Figure 8: BO-cell chip. A is condition 2.5  $\mu\text{M}$  Ro 08-2750, at day 5 after BO-cell seeding. B is condition 2.5  $\mu\text{M}$  Ro 08-2750, at day 12 after BO-cell seeding. C is condition 5ng/ml NGF, at day 5 after BO-cell seeding. D is condition 5ng/ml NGF, at day 12 after BO-cell seeding. Scale bar = 442  $\mu\text{m}$

In Figure 10 the images of an only VN-cells chip are seen of the condition 2.5  $\mu\text{M}$  Ro 08-2750 and condition 5ng/ml NGF at day 12 and 17 after VN-cell seeding. Both conditions have not a high cell density at day 12, but a higher cell density at day 17 after VN-cell seeding. Condition 5 ng/ml NGF has relatively increasing of cell density then condition 2,5  $\mu\text{M}$  RO. After day 10 the cell density decreased. At day 19 there were only a few VN-cells left in the VN-channel.

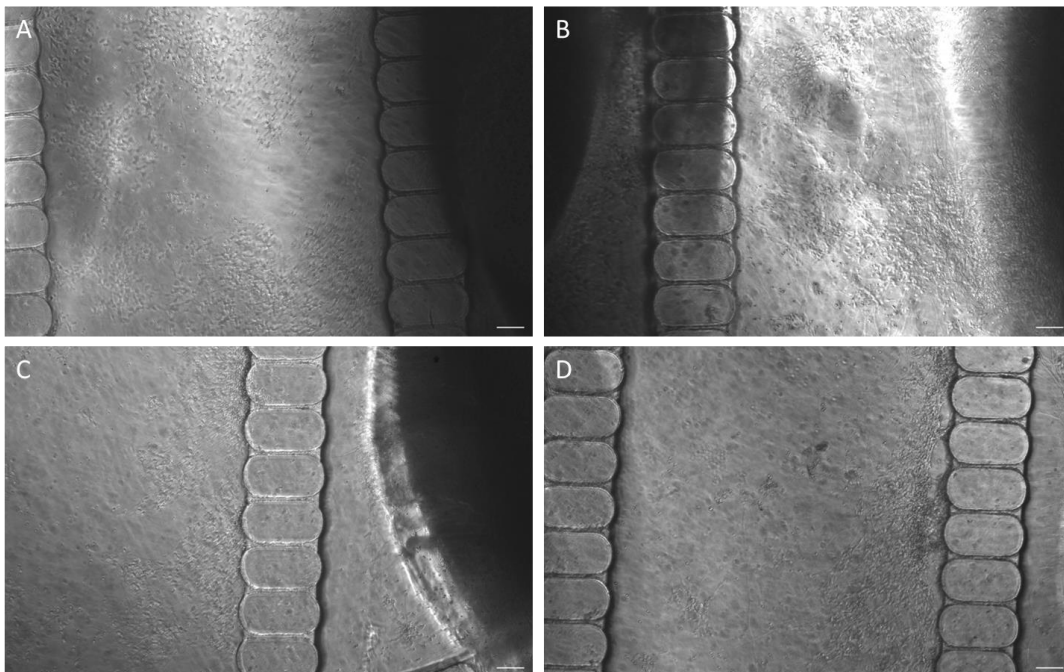


Figure 10: VN-cell chip. A is condition 5ng/ml NGF, at day 12 after VN-cell seeding. B is condition 5 ng/ml NGF at day 17 after VN-cell seeding. C is condition 2.5  $\mu\text{M}$  Ro 08-2750, at day 12 after VN-cell seeding. D is condition 2.5  $\mu\text{M}$  Ro 08-2750, at day 17 after VN-cell seeding. Scale bar = 442  $\mu\text{m}$

3.5 The immunostaining images of the HVB-chips treated with 1.0  $\mu\text{M}$  Ro 08-2750, 2.5  $\mu\text{M}$  Ro 08-2750 and 5 ng/ml NGF will be presented during the presentation of this research

Due multiple factors, the results of the immunostaining of the HVB-chips treated with 1.0  $\mu\text{M}$  Ro 08-2750, 2.5  $\mu\text{M}$  Ro 08-2750 and 5 ng/ml NGF cannot be presented in this report. These results will be presented during the presentation of this research.

## 4. Discussion

The process from chip fabrication until imaging with immunostaining was a relatively long process. Within the timeframe of this research, it was not possible to obtain all the results. The results that are not presented in this report will be discussed during the presentation of this research.

Besides the long process of the HVB-chips, there were also some other factors that caused time delay. The main reason for the time delay was that the HVB-chips with the NGF were infected with a bacterial infection. This was caused by the PBS that was used for the dilution of NGF to add it to the maintenance medium. During the next round of HVB-chips, this PBS was not used anymore to prevent another infection.

### 4.1 Microfluidic chip fabrication

For the microfluidic chip fabrication, a mold was used. This mold could only fabricate 3 chips at a time, so there were multiple fabrication steps during this research. During the process, some PDMS remained in the channels of the mold. This caused the fabricated chips to not have all the channels in it and became unusable. The mold was first cleaned with isopropanol, this did not solve the problem. After that, the channels were cleaned with a fine needle and cured with PDMS for 70 hours. After removing the PDMS, the channels were cleared, and the mold was usable again.

The bonding of the chips to the glass surface was by plasma treatment. However, during this research the Plasma System had problems due to soiling of the vacuum pump. This caused the PLO, Lamine and Fibronectin coating to not bond as expected. Because of this, the VN-cells did not attach rapidly during the latest round of HVB-chips treated with NGF and Ro 08-2750. The BO- and EB-cells could not be seeded until the VN-cells were attached, this was 5 days later. The HVB-chips also showed that the VN-cells were detached from the VN-channels 19 days after the VN-cell seeding.

### 4.2 Cell viability

The cell viability of the VN-cells was tested by different conditions of Ro 08-2750. Before this, HVB-chips were treated with 10  $\mu\text{M}$  Ro 08-2750. This condition caused a high degree of apoptosis of the VN-cells. By doing a cell viability test, the concentration with lowest degree of VN-cells apoptosis could be chosen to add to HVB-chips. As seen in Figure 3, conditions 1.0  $\mu\text{M}$  Ro 08-2750 and 2.5  $\mu\text{M}$  Ro 08-2750 normalized to VN-medium show the highest cell viability. These conditions were therefore added to the HVB-chips. Figure 3 also shows that 10  $\mu\text{M}$  Ro 08-2750 caused a relatively high degree of apoptosis. This is consistent with previous findings. The condition of 2  $\mu\text{M}$  Staurosporin expected a high degree of apoptosis,

because Staurosporine induces apoptosis. However, the incubation period of 19 hours was relatively short. This could cause the relatively lower degree of apoptosis by this condition.

### 4.3 Immunostaining EB-chips

Figure 4 shows the immunostaining images of EBs by using CTnT1 CT, CHRM2 and B-adrenergic as primary antibodies and AF488 and AF647 as secondary antibodies. These immunostainings were done to test the primary antibodies and check if the concentrations of these primary antibodies had influence on the amount of expression. For the CTnT1 CT expression, the same concentrations were used on each condition. However, condition B and C had relatively more CTnT1 CT expression. This could be caused by differences in cardiomyocyte cell types or the imaging of the confocal microscope. For the B-adrenergic expression, the lower concentration 1:100, seen in condition B, shows more expression than the higher concentration 1:50, seen in condition A. Also, for the CHRM2 expression the 1:100 concentration, seen in condition D, shows more expression than the 1:50 concentration, seen in condition C. The difference between 1:50 and 1:100 conditions are minimal, but therefore the 1:100 conditions were chosen for the HVB-chip immunostaining.

### 4.4 Immunostaining optimized HVB-chips

The first immunostaining on HVB-chips did not give an image of the BO-, VN- or EB- cells, but only a blurry image with a lot of background coloring. The cells on the HVB-chips were therefore washed and put in a clearing solution overnight. This did not solve the problem, the HVB-chips were unusable for imaging. For the next HVB-chips, the immunostaining needed to be optimized. This is done by removing the 0.1% Tween 20 from the permeabilization, blocking and antibody buffer. The presumption is that tween 20 removed not only unbound antibodies, but also bonded antibodies. This could cause the background coloring.

To check if the immunostaining was optimized, two days after cell seeding the HVB-chips were imaged. Figure 5 shows the imaging results, there is no more background coloring in each channel of the HVB-chip detected. The B-tubulin expression shows also that there has been a connection between BO- and VN- cells in Figure 5A and between EB- and VN-cells in Figure 5B. This can be used as a control in comparison with the HVB-chips treated with NGF and Ro 08-2750. HVB-chips without NGF and Ro 08-2550 also formed a (VN-BO) and (VN-EB) cellular connection. Figure 5C also shows some of the B-tubulin leaked in the channel of CTnT1 CT. This could be solved by using a lower concentration during performing the immunostaining. Figure 6 only shows the immunostaining of the EB- and VN- cells, there were no BO-cells found during imaging. This is caused by that the pipette tip, that act as medium reservoir, was not firmly fixed in the chip and fell out. By making the chip thicker, the pipette tip will stay more stable. Figure 7 shows by the expression of B-tubulin the BO-cells and cellular interaction. This image shows that there is no B-adrenergic leakage in the B-tubulin channel.

### 4.5 Brightfield microscope images of the condition 2.5 $\mu$ M Ro 08-2750 and condition 5ng/ml NGF

Figure 8 shows that the EB-cells are more bonded to the chip 12 days after EB-cell seeding. This can be seen due the formed extensions of the EBs. The BOs are also denser and more formed into steroids, this shows Figure 9.

There is not a clear difference seen between the 2.5  $\mu\text{M}$  Ro 08-2750 and condition 5ng/ml NGF due the grayscale images of the brightfield microscope. After performing immunostaining on these chips, the difference will be shown by the images of the confocal microscope.

Figure 10 shows the VN-cells in the VN-channel for the conditions 2.5  $\mu\text{M}$  Ro 08-2750 and condition 5ng/ml NGF. Both conditions show an increase in VN-cell density. However, condition 5ng/ml NGF shows a higher increase than condition 2.5  $\mu\text{M}$  Ro 08-2750. It confirms the hypothesis that NGF will promote the survival and differentiation of the VN-cells. However, this can also be confirmed by performing immunostaining.

#### 4.6 Recommendations

In this research the HVB-chips are optimized for the ventricular cardiomyocytes, hippocampal cerebral organoids and cholinergic neurons. In addition, the influence of NGF and inhibitor Ro 08-2750 is only investigated for these cell types. *In vivo*, there are multiple cell types of cardiomyocytes, cerebral organoids and neurons involved in the heart-brain connection. In further research the HVB-chips could be modeled with different types of cardiomyocytes, cerebral organoids or neurons.

## 6. Conclusion

In conclusion, there has been modeled a heart-brain connection by using OOC-technology. These HVB-chips were optimized and analyzed by immunostaining. The expression of the antibodies has shown that there is a connection between the VN-cells and the BO- and EB-cells. The influence of NGF and inhibitor Ro 08-2750 was also investigated. The bright-field microscope images show that NGF caused a higher VN-cell density than the inhibitor Ro 08-2750. However, this cannot be concluded by the bright-field microscope images. The hypotheses that NGF will promote the differentiation and cellular connection of VN-cells in HVB-chip can be confirmed or rejected by the results of the immunostaining. This result will be presented during the presentation of this research.

## References

1. Silvani A, Calandra-Buonaura G, Dampney RAL, Cortelli P. Brainheart interactions: physiology and clinical implications. *Philosophical Transactions of the Royal Society A: Mathematical, Physical and Engineering Sciences* [Internet]. 2016 May 13 [cited 2022 May 23];374(2067). Available from: <https://royalsocietypublishing.org/doi/full/10.1098/rsta.2015.0181>
2. Chapter 01: Heart-Brain Communication | HeartMath Institute [Internet]. [cited 2022 May 24]. Available from: <https://www.heartmath.org/research/science-of-the-heart/heart-brain-communication/>
3. Bekijk de cijfers over hart- en vaatziekten | Hartstichting [Internet]. [cited 2022 May 31]. Available from: <https://www.hartstichting.nl/hart-en-vaatziekten/feiten-en-cijfers-hart-en-vaatziekten>
4. Cijfers over patiënten - Hersenstichting [Internet]. [cited 2022 May 31]. Available from: <https://www.hersenstichting.nl/cijfers-over-patienten/>
5. Hooghiemstra AM, Bertens AS, Leeuwis AE, Bron EE, Bots ML, Brunner-La Rocca HP, et al. The Missing Link in the Pathophysiology of Vascular Cognitive Impairment: Design of the Heart-Brain Study. *Cerebrovasc Dis Extra* [Internet]. 2017 Oct 2 [cited 2022 May 24];7(3):140–52. Available from: <https://pubmed.ncbi.nlm.nih.gov/29017156/>
6. Hooghiemstra AM, Leeuwis AE, Bertens AS, Biessels GJ, Bots ML, Brunner-La Rocca HP, et al. Frequent Cognitive Impairment in Patients With Disorders Along the Heart-Brain Axis. *Stroke* [Internet]. 2019 Dec 1 [cited 2022 May 24];50(12):3369–75. Available from: <https://pubmed.ncbi.nlm.nih.gov/31684846/>
7. Koppikar S, Baranchuk A, Guzmán JC, Morillo CA. Stroke and ventricular arrhythmias. *Int J Cardiol* [Internet]. 2013 Sep 30 [cited 2022 Jul 5];168(2):653–9. Available from: <https://pubmed.ncbi.nlm.nih.gov/23602297/>
8. Ruthirago D, Julayanont P, Tantrachoti P, Kim J, Nugent K. Cardiac Arrhythmias and Abnormal Electrocardiograms After Acute Stroke. *The American Journal of the Medical Sciences* [Internet]. 2016 Jan 1 [cited 2022 Jul 5];351(1):112–8. Available from: <http://www.amjmedsci.org/article/S000296291500018X/fulltext>
9. Zhu Z, Huangfu D. Human pluripotent stem cells: an emerging model in developmental biology. *Development* [Internet]. 2013 Feb 2 [cited 2022 Jul 4];140(4):705. Available from: </pmc/articles/PMC3557771/>
10. Schwach V, Cofiño-Fabres C, Den SA ten, Passier R. Improved Atrial Differentiation of Human Pluripotent Stem Cells by Activation of Retinoic Acid Receptor Alpha (RAR $\alpha$ ). *Journal of Personalized Medicine* [Internet]. 2022 Apr 13 [cited 2022 May 31];12(4):628. Available from: </pmc/articles/PMC9032956/>
11. Andrysiak K, Stępniewski J, Dulak J. Human-induced pluripotent stem cell-derived cardiomyocytes, 3D cardiac structures, and heart-on-a-chip as tools for drug research. *Pflugers Archiv* [Internet]. 2021 Jul 1 [cited 2022 Jun 16];473(7):1061. Available from: </pmc/articles/PMC8245367/>
12. Kapałczyńska M, Kolenda T, Przybyła W, Zajączkowska M, Teresiak A, Filas V, et al. 2D and 3D cell cultures – a comparison of different types of cancer cell cultures. *Archives of Medical*

- Science : AMS [Internet]. 2018 [cited 2022 Jul 5];14(4):910. Available from: [/pmc/articles/PMC6040128/](#)
13. Zhu J, Zhu J. Application of Organ-on-Chip in Drug Discovery. *Journal of Biosciences and Medicines* [Internet]. 2020 Mar 2 [cited 2022 Jul 5];8(3):119–34. Available from: <http://www.scirp.org/journal/PaperInformation.aspx?PaperID=98810>
  14. Zheng F, Fu F, Cheng Y, Wang C, Zhao Y, Gu Z. Organ-on-a-Chip Systems: Microengineering to Biomimic Living Systems. *Small* [Internet]. 2016 May 4 [cited 2022 Jul 4];12(17):2253–82. Available from: <https://pubmed.ncbi.nlm.nih.gov/26901595/>
  15. Brofiga M, Pisano M, Raiteri R, Massobrio P. On the road to the brain-on-a-chip: a review on strategies, methods, and applications. *Journal of Neural Engineering* [Internet]. 2021 Aug 12 [cited 2022 Jun 21];18(4):041005. Available from: <https://iopscience.iop.org/article/10.1088/1741-2552/ac15e4>
  16. Aloe L, Rocco ML, Balzamino BO, Micera A. Nerve growth factor: role in growth, differentiation and controlling cancer cell development. *Journal of Experimental & Clinical Cancer Research : CR* [Internet]. 2016 Jul 21 [cited 2022 Jun 8];35(1). Available from: [/pmc/articles/PMC4955168/](#)
  17. Fischer W, Wictorin K, Björklund A, Williams LR, Varon S, Gage FH. Amelioration of cholinergic neuron atrophy and spatial memory impairment in aged rats by nerve growth factor. *Nature* [Internet]. 1987 [cited 2022 Jun 28];329(6134):65–8. Available from: <https://pubmed.ncbi.nlm.nih.gov/3627243/>
  18. Levi-Montalcini R, Hamburger V. Selective growth stimulating effects of mouse sarcoma on the sensory and sympathetic nervous system of the chick embryo. *J Exp Zool* [Internet]. 1951 [cited 2022 Jun 28];116(2):321–61. Available from: <https://pubmed.ncbi.nlm.nih.gov/14824426/>
  19. Govoni S, Pascale A, Amadio M, Calvillo L, D’Elia E, Cereda C, et al. NGF and heart: Is there a role in heart disease? *Pharmacological Research*. 2011 Apr 1;63(4):266–77.
  20. Niederhauser O, Mangold M, Schubanel R, Kuszniir EA, Schmidt D, Hertel C. NGF Ligand Alters NGF Signaling Via p75 NTR and TrkA. *J Neurosci Res*. 2000;61:263–72.
  21. Zhang L, Jiang H, Hu Z. Concentration-dependent effect of nerve growth factor on cell fate determination of neural progenitors. *Stem Cells Dev* [Internet]. 2011 Oct 1 [cited 2022 Jul 4];20(10):1723–31. Available from: <https://pubmed.ncbi.nlm.nih.gov/21219132/>
  22. Schwach V, Cofiño-Fabres C, Den SA ten, Passier R. Improved Atrial Differentiation of Human Pluripotent Stem Cells by Activation of Retinoic Acid Receptor Alpha (RAR $\alpha$ ). *Journal of Personalized Medicine* [Internet]. 2022 Apr 13 [cited 2022 May 10];12(4):628. Available from: [/pmc/articles/PMC9032956/](#)
  23. Ribeiro MC, Slaats RH, Schwach V, Rivera-Arbelaez JM, Tertoolen LGJ, van Meer BJ, et al. A cardiomyocyte show of force: A fluorescent alpha-actinin reporter line sheds light on human cardiomyocyte contractility versus substrate stiffness. *Journal of Molecular and Cellular Cardiology* [Internet]. 2020 Apr 1 [cited 2022 Jul 4];141:54–64. Available from: <http://www.jmcc-online.com/article/S0022282820300699/fulltext>

24. Sakaguchi H, Kadoshima T, Soen M, Narii N, Ishida Y, Ohgushi M, et al. Generation of functional hippocampal neurons from self-organizing human embryonic stem cell-derived dorsomedial telencephalic tissue. *Nature Communications* 2015 6:1 [Internet]. 2015 Nov 17 [cited 2022 Jul 4];6(1):1–11. Available from: <https://www.nature.com/articles/ncomms9896>
25. Goldsteen PA, Sabogal Guaqueta AM, Bos IST, Kistemaker LEM, van der Koog L, Eggens M, et al. Differentiation of airway cholinergic neurons from human pluripotent stem cells for airway neurobiology studies. *bioRxiv* [Internet]. 2022 Mar 26 [cited 2022 Jul 6];2022.03.23.485449. Available from: <https://www.biorxiv.org/content/10.1101/2022.03.23.485449v1>
26. Poly-L-Ornithine Solution (0.01%) | Sigma-Aldrich [Internet]. [cited 2022 May 30]. Available from: <https://www.sigmaaldrich.com/NL/en/product/mm/a004m>
27. Mousa SA. Cell adhesion molecules: Potential therapeutic & diagnostic implications. *Molecular Biotechnology*. 2008 Jan;38(1):33–40.
28. CellTiter-Glo® 2.0 Assay Protocol [Internet]. [cited 2022 Jul 7]. Available from: <https://nld.promega.com/resources/protocols/technical-manuals/101/celltiterglo-2-0-assay-protocol/>
29. Vagal Maneuvers: How To Slow Your Heart Rate [Internet]. [cited 2022 May 23]. Available from: <https://my.clevelandclinic.org/health/treatments/22227-vagal-maneuvers>